5.2 A NEW COMPOSITE OBSERVING SYSTEM STRATEGY FOR GROUND-BASED GPS METEOROLOGY

Seth I. Gutman*[1], Susan Sahm[1], Jebb Stewart[2], Stan Benjamin[1], Tracy Smith[3], and Barry Schwartz[1]

[1]NOAA Forecast Systems Laboratory, Boulder, Colorado
[2]Systems Research Group (SRG) Inc., Boulder Colorado
[3]Colorado State University/CIRA, Ft. Collins, Colorado

1. INTRODUCTION

The current implementation of ground-based GPS meteorology (GPS-Met) at the NOAA Forecast Systems Laboratory involves the retrieval of total column precipitable water vapor from excess delays in the Global Positioning System radio signals caused by the refractivity of the neutral (non-dispersive) atmosphere, primarily the troposphere. The total excess signal delay is defined as:

$$TD = \int n(s)ds \qquad (1)$$

where $n(s)$ is the index of refraction along the line-of-sight signal path from the GPS antenna to the satellite. The tropospheric signal delay is estimated by forming an "ionospheric free" carrier phase observation (M_{IF}) to eliminate the impact of the ionosphere (Equation 2), and then forming a "double-difference" (DD) to remove receiver and satellite clock biases as illustrated in Figure 1.

$$M_{IF} \cong 2.546\ M_{L1} - 1.984\ M_{L2} \qquad (2)$$

We assume that tropospherically induced signal delays depend primarily on satellite elevation above the horizon (as opposed to azimuth) since the former determines the length of the path through the atmosphere. We also assume that the total delay has only a wet and dry component. The GPS signal delay along a single path $TD(")$ is then modeled in terms of an unknown "zenith tropospheric delay" (ZTD) and known elevation angle-dependent mapping functions for the wet and dry delays m_W and m_D as defined in Equation 3 (Neill, 1996) .

$$TD(") = m_D(")*ZTD + m_W(")*ZTD \qquad (3)$$

*Corresponding author address: Seth I. Gutman, NOAA Forecast Systems Laboratory, 325 Broadway R/FS3, Boulder, CO 80305-3328, gutman@fsl.noaa.gov, http://gpsmet.noaa.gov.

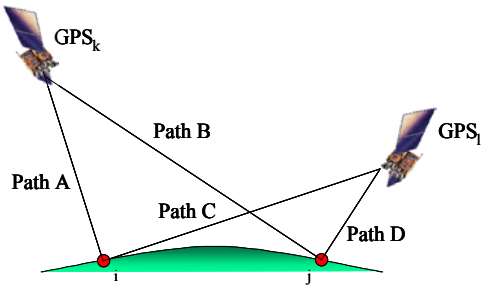

Figure 1. Forming a double difference from ionospheric free carrier phase GPS observations.

Since there are 6-10 GPS satellites at different elevations in view at all times, solutions for the ZTD are over-determined and can be estimated with high accuracy as a nuisance parameter in a relative or absolute sense (Mikhail, 1976). Duan et al. (1996) described a technique whereby ZTD can be estimated in an absolute sense at each station in a network of continuously operating GPS reference stations.

2. RETRIEVAL OF WATER VAPOR FROM GPS SIGNAL DELAYS

The wet and dry components of total refractivity are described in Equation 4.

$$N = 77.6\frac{P_d}{T} + 70.4\frac{P_v}{T} + 3.739\frac{P_v}{T^2} \qquad (4)$$

where: N = total refractivity = (n-1)x10^6
P_d = atmospheric pressure (hPa)
P_v = water vapor pressure (hPa)
T = temperature.

The dry or hydrostatic component (the left-most term on the right side of the equation) is caused by the mass of the neutral atmosphere, and is directly proportional to the atmospheric pressure at the height of the GPS antenna. The wet component is caused by the dipole moments

of the water vapor molecules along the paths of the GPS signals (Bevis et al., 1992). The wet refractivity has two terms that include the water vapor mixing ratio q, and q/T.

The separation of the tropospheric delay into its wet and dry components, and retrieval of integrated (total column) precipitable water vapor (IPW) is carried out in a straightforward manner as follows:

- calculate the zenith hydrostatic or "dry" delay (*zhd*) from the atmospheric pressure using the Saastamoinen (1972) formulation;
- subtract the zenith hydrostatic delay (*zhd*) from the *ztd* using the technique described above to derive the zenith wet delay (*zwd*);
- map the zenith wet delay into IPW through a mapping function that is inversely proportional to T_m, the water vapor weighted mean temperature of the atmosphere (Bevis et al., 1992).

Rather than interpreting GPS IPW retrievals as point measurements at discrete times, they should be as a volume averages over the region of the sky covered by the satellite constellation in 30 minutes. Given the current configuration of the GPS constellation, the region sampled has a radius of about 11 kilometers, and the averaging period is now seen as essentially arbitrary.

As a consequence, GPS IPW retrievals have much in common with satellite and rawinsonde TPW observations. The major exceptions include: GPS-Met is an all weather remote sensing technique that is not hindered by clouds or precipitation; the accuracy is comparable to integrated rawinsonde moisture observations, but with higher precision and temporal resolution; the measurement requires no calibration; and the accuracy does not degrade with time since it depends on atomic clocks with constantly improving accuracy. The principle shortcoming of GPS-Met is that it is an integrated measurement that provides (in itself) no information about the vertical distribution of moisture above the sites.

The accuracy of any observing system, including GPS, is determined by comparing its observations with measurements made by other independent observing systems whose characteristics are well known. Figure 2 is a comparison of clear sky water vapor observations made during a three-week period in the early Fall of 2000 by eight different observing systems at the DOE ARM CART Site in North Central Oklahoma. Figure 3 is a scatter plot of sonde versus GPS water vapor retrievals for this experiment. The mean difference for 114 comparisons is 0.074 cm IPW, the standard deviation is 0.123 cm IPW, and the correlation coefficient is 0.99272.

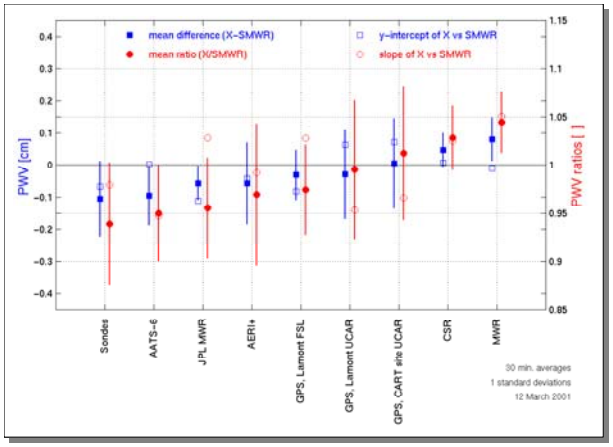

Figure 2. Water vapor observations made during the water vapor intensive observing period at the DOE ARM CART Site in North Central Oklahoma, September 18 – October 9, 2000. All observing systems are compared to a spare microwave water vapor radiometer (SMWR) deployed at the site during the campaign.

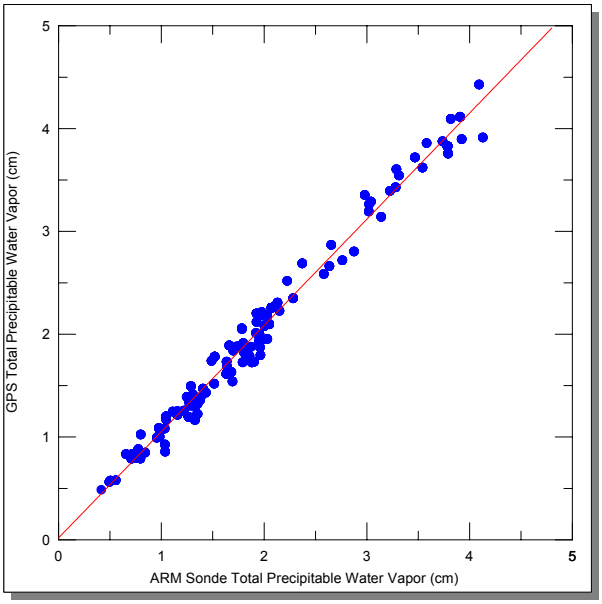

Figure 3. Rawinsonde vs. GPS water vapor observations during the 2000 Water Vapor Intensive Observing Period in 2000.

To demonstrate that GPS-Met observations can be carried out virtually anywhere, Figure 4 shows a recent comparison of GPS retrievals and

rawinsonde measurements made at the Blacksburg, VA Weather Service Forecast Office.

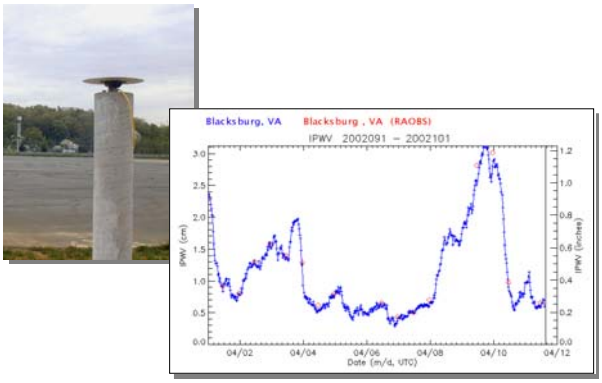

Figure 4. Comparison of GPS IPW retrievals and rawinsonde measurements made at the Blacksburg Virginia Weather Service Forecast Office in April, 2002. The GPS is located adjacent to the rawinsonde inflation shelter at the Blacksburg airport on the campus of Virginia Tech.

3. IMPROVEMENTS IN FORECAST ACURACY

The evaluation of utility of GPS-Met data in subjective forecasting is just beginning, but the initial reactions of NWS Science and Operations Officers and duty forecasters is that it can provide very valuable information under a wide range of conditions (personal communications with P. Welsh, L. Dunn, S. Keighton, P. Santos, and others).

In contrast, evaluations of the impact of GPS water vapor observations on numerical weather forecast accuracy have been carried out at FSL since 1998. The hypothesis tested was that even in the conterminous United States, one of the most well observed regions on Earth, improvements in moisture and precipitation forecast accuracy are still possible because water vapor at meso-alpha and smaller scale is under observed in time and space. For example, the GOES sounders provide no temperature or moisture information under cloudy conditions associated with severe weather when, in general, it is needed most.

Even though GPS-Met provides no direct information about the vertical distribution of moisture in the atmosphere, it still provides an accurate total column measurement under all weather conditions and climates.

Techniques to assimilate GPS IPW retrievals into mesoscale numerical weather prediction models such as the Rapid Update Cycle (RUC) have been developed and tested with gratifying results. Continuous improvements in short-range moisture and precipitation forecast accuracy have been observed since parallel (i.e. with and without GPS-Met) runs began in 1997 (Benjamin et al., 1998; Smith et al., 1999, 2000, 2002; Gutman et al., 2001). Figure 5 shows improvements in 3-hour precipitation forecast skill in 2000 and 2001. Data denial experiments were conducted using the FSL version of the RUC that assimilates all observations including GPS IPW data. Verification is against the NCEP 24-hour precipitation product.

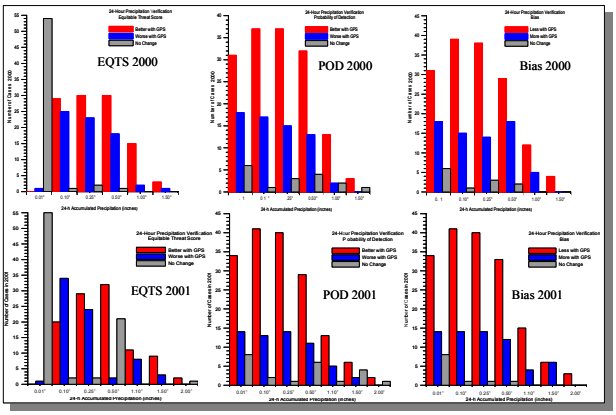

Figure 5. 3-hour precipitation forecast verification statistics for 2000 and 2001. In each bar chart, the color red represents an improvement in forecast skill, blue is worse skill, and gray is no change. The metrics are equitable threat score (EQT), probability of detection (POD) and bias. In general, improvement is observed at all levels of precipitation above 0.01" in 2000, and above 0.1" in 2001.

One of the most definitive results thus far is that the impact on forecast accuracy increases as the network of GPS-Met observing systems expands. This result is both reasonable and obvious, given the temporal and spatial variability of water vapor in the lower atmosphere, and the fact that water vapor is under-observed in both time and space, especially during active weather.

This result has evoked two questions: what is the minimum number and distribution of GPS-Met observing systems needed to provide complementary moisture observations without unnecessary redundancy; and what is the best way to expand the GPS-Met coverage at the lowest possible cost without sacrificing data quality, system reliability, and maintainability?

4. OBSERVING SYSTEM STRATEGIES

The answer to the first question depends on the application. As an element of a composite

upper-air observing system using complementary measurements from rawinsondes, satellites, radars, and commercial aircraft, the average station spacing would be about least 100 km. If techniques to measure and validate line of sight signal delays can be developed, than the station spacing should be on the order of 40-km (MacDonald et al., 2000), In either case, this should allow us to continuously capture meso-alpha scale moisture structure under all weather conditions. GPS IPW observations should be made at every forecast office, upper-air facility, and major airport as validation for moisture soundings. Stations in between these sites will provide data continuity during asynoptic periods. As an element of the global climate observing system, GPS-Met systems should be spread out along the coasts, on islands in the ocean basins, in other remote locations, and at key facilities such as climate observatories. One application of GPS-Met that is being explored at FSL is the use of brightness temperatures derived from GPS wet refractivity measurements to provide calibration and validation for satellite or aircraft remote sensing observations, and for inter-platform calibration of temperature and moisture retrievals from radiometers.

The answer to the second question involves tradeoffs between system acquisition, installation, operation and maintenance costs and data quality, reliability, and maintainability. In recent years, federal, state and local government agencies, universities and private companies have established networks of continuously operating GPS reference stations for the purpose of improving positioning and navigation services for a wide variety of applications and users (Gutman et al., 2003). Due to a fortuitous synergy between the instrument requirements for high accuracy positioning and those of GPS-meteorology, it is possible to use these other systems for weather forecasting if the data are available in near real-time. The problem is that since high accuracy positioning does not necessarily require collocated surface meteorological observations, and GPS-Met does, few if any of these CORS sites have met sensors or the data is not collected.

To take advantage of GPS-only observations for GPS-Meteorology, we investigated operational techniques to use surface meteorological observations from other sources to parse the signal delays into their wet and dry components. The remainder of this paper discusses the methods used to do this and the expected errors associated with this process. The result is a new observing system strategy for building GPS-Met networks.

We define two classes of GPS observing systems: one called a “Backbone site” and the other called a “Infill site”. The distinction between the two is that backbone sites are usually owned, operated, and maintained by federal government agencies as operational systems. Each backbone site has a collocated surface meteorological sensor package, reliable power, and dedicated or reliable communications. Infill sites are not maintained as operational systems, and may or may-not have collocated meteorological sensors or dedicated communications.

The goal is to have backbone sites more or less evenly distributed across the United States and use infill sites to densify the network. The current implementation of this strategy is illustrated in Figure 6.

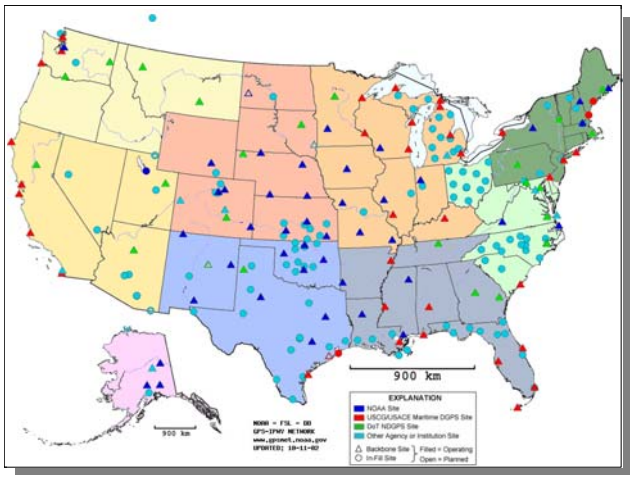

Figure 6. NOAA GPS-Met Demonstration Network as of 10-11-02. Triangles indicate the locations of backbone sites, while circles are infill sites. Colors identify the owners as: NOAA (dark blue), U.S. Coast Guard (red), U.S. Department of Transportation (green), other agency or institution (light blue).

5. RETRIEVING WATER VAPOR AT INFILL SITES

Surface Pressure at Infill Sites. How far can a pressure measurement be made from the GPS antenna and still be used to separate the wet and dry components of the tropospheric signal delay with sufficient accuracy to improve weather forecast accuracy? The answer ultimately depends on the horizontal and vertical pressure gradient. Under conditions of hydrostatic equilibrium:

$\frac{\partial p}{\partial x}\delta x$ and $\frac{\partial p}{\partial y}\delta y$ (5) are negligible, and

$\frac{\partial p}{\partial z}\delta z = -g\rho$ (6) dominates.

Even under non-hydrostatic conditions, when the horizontal pressure gradient is significant and local wind flow is high, the impact (while important) tends to be spatially localized and relatively short-lived.

To quantify the relationships between pressure interpolation accuracy and horizontal and vertical distance, we performed a series of studies in which the atmospheric pressure measured at a GPS site using the GPS Surface Observing System (GSOS) barometer (with known error characteristics) was compared with pressure interpolated vertically from the altimeter setting at the nearest ASOS site. To do this, we used the standard equation from the National Weather Service Training Center ASOS Algorithm Tutorial, see:
http://meted.ucar.edu/export/asos/Pressure.HTML

$$P_{sfc} = \left[Alt^{0.193} - (1.313 \times 10^{-5}) \times ele \right]^{5.255} \quad (7)$$

This method of interpolation was selected over other methods to avoid the pressure errors introduced by biases in modeled terrain that could exceed our threshold of 1 hPa by a significant factor. These biases arise from the differences between the average elevation in a model grid cell and the actual elevation as illustrated in Table 1 from Benjamin et al., (2002).

The sites used in this study were selected in coastal, Great Plains, and mountain environments to sample different climatological regions. The study was carried out during two months in the Winter of 2001 and repeated in the late Spring of 2002 to evaluate the impact of different weather conditions and seasonal variations on local pressure. A total of 24,085 comparisons were made at 17 sites during the winter, and 14,243 at 13 sites during the spring. The ASOS and GPS units were separated by 3 km to 53 km horizontally, and 2 meters to 200 meters vertically, as detailed in Table 2.

Figure 7 is a histogram of the standard deviations of the differences between interpolated ASOS pressure and GSOS measurements during the winter and spring. Figure 8 is a scatter plot of interpolated ASOS versus GSOS measurements during both periods.

Rawinsonde station	**Station elevation minus RUC20 elevation (m)**
Edwards AFB, CA	41
Denver, CO	26
Grand Junction, CO	323
Boise, ID	253
Great Falls, MT	29
Reno, NV	144
Elko, NV	152
Medford, OR	346
Salem, OR	51
Rapid City, SD	45
Salt Lake City, UT	438
Riverton, WY	119

Table 1. Terrain elevation difference between station elevation and interpolated RUC elevation for selected rawinsonde stations in western United States. Unless corrected, these differences will introduce large pressure errors resulting in significant GPS-Met retrieval errors.

Spring	Largest	Mean	Std. Dev.	Baseline	Elevation	Number
BIL1	2.17	0.466	0.509934	45.9737	200.2293	1320
CCV3	-2.62	-0.231	0.337839	27.5336	2.9034	896
CHA1	-1.3	-0.201	0.282577	23.6144	10.1961	1289
DSRC	-4.88	-0.288	0.550783	52.9511	14.8671	1302
FST1	-1.23	-0.418	0.245537	16.4906	20.1364	1297
GAL1	1.68	0.117	0.322351	14.0083	6.242	1313
MC01	-2.2	-0.173	0.304955	3.2562	20.7845	1179
MOB1	-1.67	0.056	0.336304	44.1651	11.1189	1270
PLTC	-3.8	1.002	0.601011	36.7029	136.0323	1148
SAV1	1.83	0.137	0.388089	46.694	23.073	1291
SEAW	1.2	-0.057	0.31972	27.4506	119.1421	1325
SPN1	-2.48	-0.405	0.309252	13.874	17.3571	1308
SYCN	1.28	0.413	0.250045	1.3175	2.8596	1305

Winter	Largest Number	Mean	Std. Dev.	Baseline	Elevation	
BIL1	-3.5	-1.1863	0.7283	45.9737	200.2293	1324
CCV3	-2.1	-0.1881	0.25325	27.5336	2.9034	1019
CHA1	1.7	-0.3244	0.3207	23.6144	10.1961	1477
DET1	2.2	-0.0105	0.29634	14.1081	11.2758	1530
DSRC	2.9	-0.2158	0.4262	52.9511	14.8671	1398
FST1	-1.8	-0.7202	0.2673	16.4906	20.1364	1582
GAL1	3.1	0.0907	0.2737	14.0083	6.242	1475
HAG1	-2.4	-0.6908	0.3616	16.8975	68.8088	1427
MC01	-1.5	-0.6498	0.1771	3.2562	20.7845	1469
MCD1	1.7	-0.2247	0.1792	3.181	7.72	1249
MOB1	3.4	0.1611	0.42695	44.1651	11.1189	1502
PLTC	1.7	0.0493	0.4566	36.7029	136.0323	1285
PUB1	-1.6	-0.6374	0.229	12.741	3.9668	1312
SAV1	2.1	-0.06867	0.36784	46.694	23.073	1350
SEAW	2.4	-0.4057	0.5062	27.4506	119.1421	1495
SLCU	-1.8	-0.2425	0.2067	2.2092	4.7417	1877
SPN1	-1.9	-0.4888	0.3252	13.874	17.3571	1495
SYCN	-2	0.2335	0.2356	1.3175	2.8596	1696

Table 2. Sites used in the experiments in spring (top) and winter (bottom). Columns from left to right are: Site ID, largest difference (hPa), mean difference (hPa), std. Deviation (hPa), horizontal offset, vertical offset, and number of comparisons.

The next step is to determine the relationship between the pressure outliers (i.e. hPa deviations greater than one sigma) and vertical and horizontal baseline difference. The results of these analyses are presented in Figures 9 and 10.

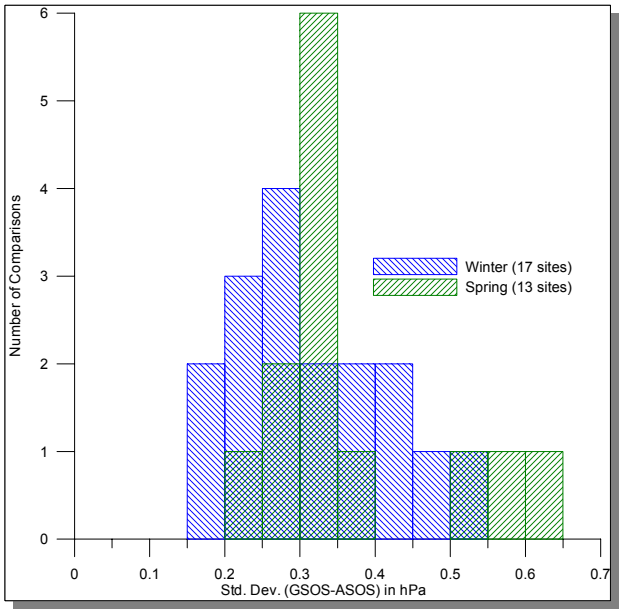

Figure 7. Histogram of standard deviations of differences between interpolated ASOS pressure and GSOS measurements.

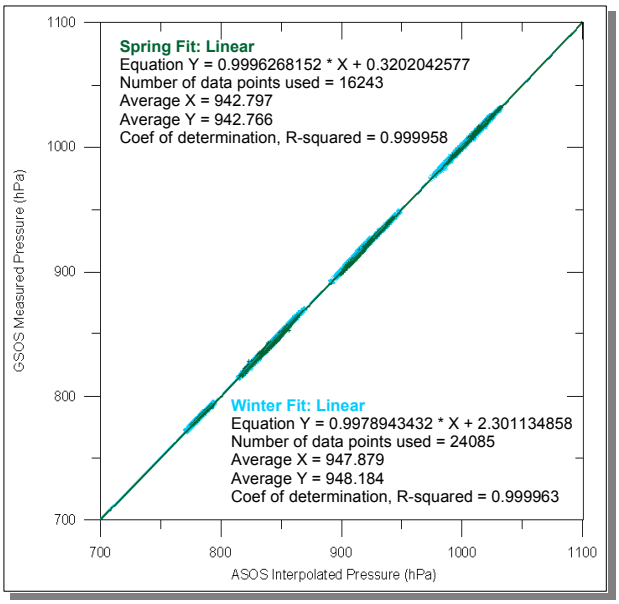

Figure 8. Scatter plot of all data. Winter mean and standard deviation are –0.31 hPa and 0.523 hPa, respectively. Spring mean and standard deviation are 0.03 hPa and 0.540 hPa.

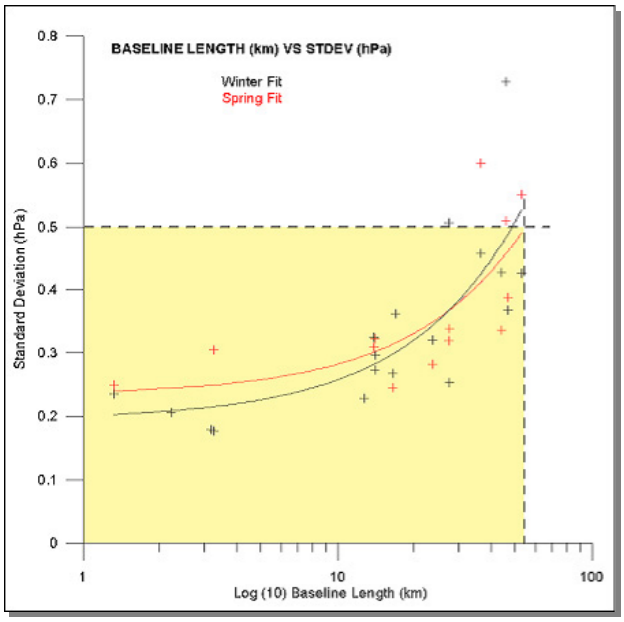

Figure 9. Baseline length (km) versus pressure variance (hPa) for all sites. Bias corrected pressure measurements made within 50 km of a CORS site can be used for GPS-Met with high confidence.

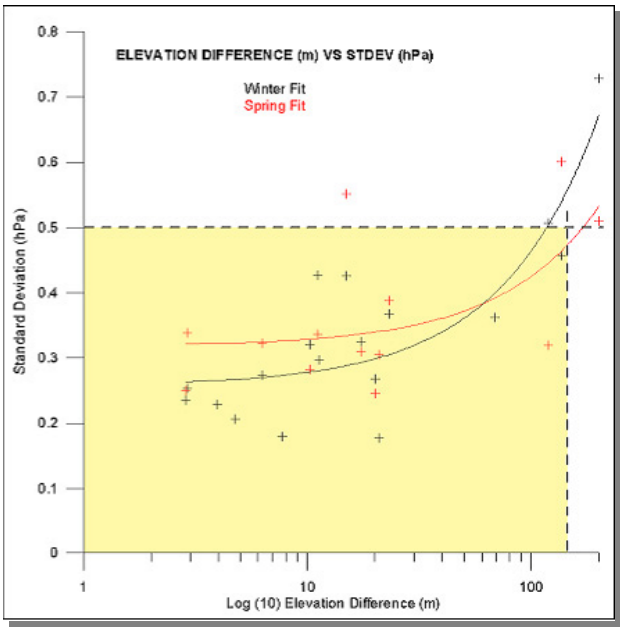

Figure 10. Elevation difference (m) versus pressure variance (hPa) for all sites. Bias corrected pressure measurements made within 100 m of a CORS site can be used for GPS-Met with high confidence.

As indicated in Figures 9 and 10, the slope in the biases (i.e. differences between the pressure observations and interpolated values as a function of horizontal and vertical distance) are relatively flat out to about 25 km horizontal and 20 m vertical respectively, and appear to increase exponentially thereafter. The magnitude of the "close in" bias is between 0.2 and 0.3 hPa, and increases to about 0.5 hPa at around 50 km horizontal and 100 m vertical. This is consistent with comparisons between pressure observations at Platteville, Colorado (PLTC) and interpolated values derived from the ASOS at Denver International Airport (KDEN) shown in Figure 11. The offsets of these sites are 36.7 km horizontal and 136 m vertical.

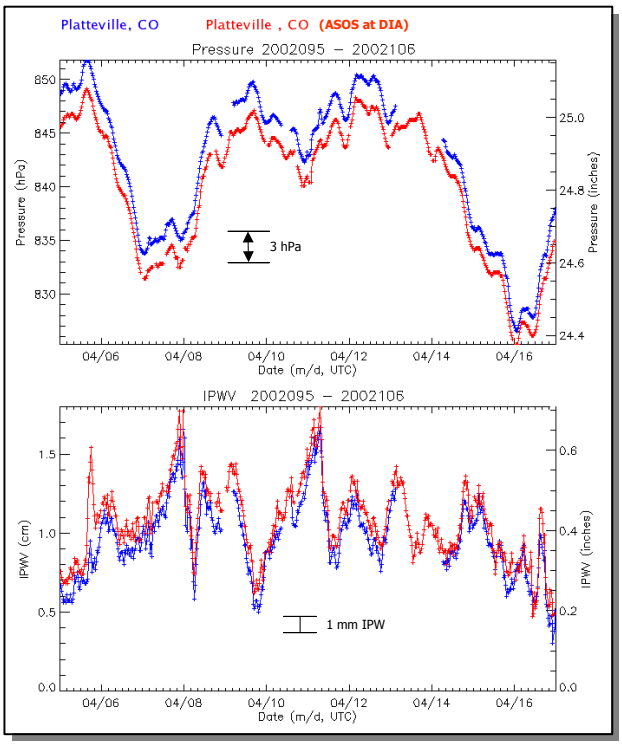

Figure 11. Comparison of observed pressure at Platteville, CO (PLTC) and interpolated pressure from KDEN (37 km west and 136 m higher) over 10 days in 2002. The -3 hPa average bias is sufficient to account for the +1 mm IPW bias observed in the lower panel.

We examined several methods to correct the residual biases in interpolated pressure, and rejected empirical techniques because they could not reliably account for seasonal to intra-annual changes in the biases (Figure 8). We believe that there are at least two causes for the changes: normal seasonal variations and instrument drift.

We then evaluated the statistical characteristics of a data assimilation system such as the Mesoscale Analysis and Prediction System (MAPS) - Rapid Update Cycle (RUC) Surface Assimilation Systems (MSAS/RSAS) described in Miller et al., (in preparation). A description of the MSAS/RSAS Surface Analysis is available at http://www-sdd.fsl.noaa.gov/MSAS/msas_descrip.html.

We determined that since the mean MSAS/RSAS analysis error was essentially zero regardless of season, we could effectively use it as the basis for a pressure bias correction at those infill sites without surface meteorological sensors.

The correction is carried out as follows. Given an automated surface observing system within 50 km horizontal and 100 meters vertical of a CORS site:

- Determine the observed mean daily altimeter setting value at the nearest ASOS for the previous day.
- Compare that with the mean MSAS/RSAS altimeter setting for the previous day at the location of the infill site using bilinear interpolation from the model grid.
- Apply the difference to the interpolated pressure at the height of the GPS antenna.
- Use that value to calculate the zenith hydrostatic signal delay as described in Saastamoinen (1972).

Mean Temperature at Infill Sites. The water vapor weighted mean temperature of the atmosphere, T_m, is calculated using parameters derived from a mesoscale numerical model using the equation:

$$T_m = \frac{\int \frac{P_v}{T} dz}{\int \frac{P_v}{T^2} dz} \qquad (8)$$

rather than a regression algorithm (Bevis et al., 1992, or Ross and Rosenfeld, 1997) based on global rawinsonde observations. Figure 12 is a comparison between T_m calculated from surface temperature measurements using the Bevis algorithm (Bevis et al., 1992), independent observations using an AERI radiometer from the University of Wisconsin during a field campaign in Louisville, KY in 1999 (D. Tobin, personal communication), and the RUC numerical weather prediction model.

The average difference between Bevis T_m estimates and the AERI retrievals is about 5^o K, quite close to the error estimate of Bevis et al., 1992. Most of the scatter in the Bevis estimate appears to come from the diurnal variation in

surface temperature that is not strongly represented in either the measurements or analyses. Finally, the differences between AERI retrievals and RUC T_m analysis are less than 1%.

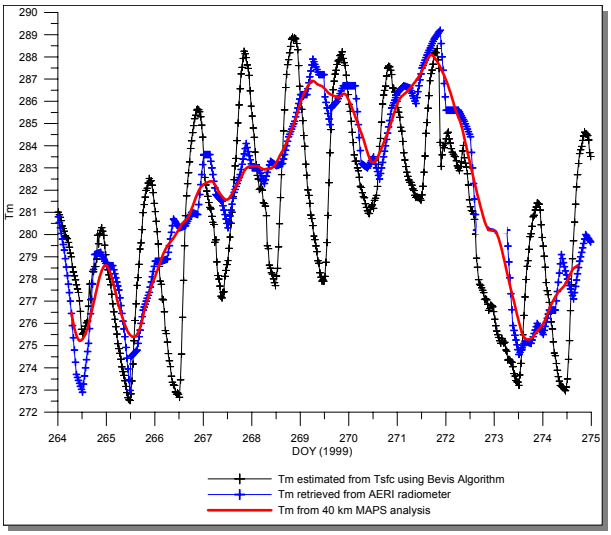

Figure 12. Comparison between water vapor weighted mean temperature of the atmosphere (T_m) calculated from surface temperature (Bevis et al., 1992), observations using an AERI radiometer from the University of Wisconsin, and the FSL RUC.

6. CONCLUSIONS

The highest accuracy GPS retrievals of integrated precipitable water vapor are made when accurate surface temperature and pressure measurements are made at GPS continuously operating reference stations. When maintained as operational systems by federal agencies such as NOAA, USCG, or DOT, these sites are referred to as "Backbone Sites" in the ground-based GPS-Met network established by NOAA's Forecast Systems Laboratory. Backbone sites provide the most accurate and upper-air moisture observations to forecasters and modelers with high reliability under all weather conditions.

The rapid proliferation of GPS continuously operating reference stations sites by federal, state and local government agencies, universities, and the private sector primarily for positioning and navigation applications, provides NOAA with an extraordinary opportunity to expand the coverage of GPS-Met sensors across the nation at very low cost. By combining these GPS observations with independent observations made at nearby automated surface observing systems such as ASOS and Road Weather Information Systems (RWIS) using the schema described in this paper, NOAA will be able to use them as "Infill Sites" to further expand and densify the nationwide coverage of GPS-Met observing systems.

This is important because the impact of GPS-Met on objective weather forecast accuracy is strongly linked to the number of observations. In addition, the subjective use of these data will be greatly enhanced when reasonably dense local GPS networks permit the moisture associated with severe weather and heavy precipitation to be tracked simultaneously by several observing systems in a complementary fashion.

7. ACKNOWLEGEMENTS

The authors wish to acknowledge the contributions of numerous individuals to this study, including Kirk Holub of the FSL Demonstration Division, Patty Miller and Mike Barth of the FSL Systems Development Division, Ara Howard of the FSL Information and Technology Services group, Dave Tobin at the University of Wisconsin, the DOE Atmospheric Radiation Measurement Program, and Stephen Keighton of the National Weather Service at Blacksburg, VA.

8. REFERENCES

Benjamin, S., T. Smith, B. Schwartz, S. Gutman, and D. Kim, 1998: Precipitation forecast sensitivity to GPS precipitable water observations combined with GOES using RUC-2. 2nd Symp. on Int. Obs. Sys., AMS, Phoenix, AZ.

Benjamin, S.G., J.M. Brown, K.J. Brundage, D. Dévényi, G.A. Grell, D. Kim, B.E. Schwartz, T.G. Smirnova, T.L. Smith, S.S. Weygandt, and G.S. Manikin, 2002. RUC20 - The 20-km version of the Rapid Update Cycle, NWS Technical Procedures Bulletin No. 490, 11 April 2002 (updated 16 May).

Bevis M., S. Businger, T.A. Herring, C. Rocken, R.A. Anthes and R.H. Ware, 1992. GPS meteorology: remote sensing of atmospheric water vapor using the Global Positioning System, *J. Geophys. Res.,* 97, 15787-15801.

Duan, J.M., M. Bevis, P. Fang, Y. Bock, S.R. Chiswell, S. Businger, C. Rocken, F. Soldheim, R.H. Ware, T.A. Hering, and R.W. King, 1996. Remote Sensing Atmospheric Water Vapor using the Global Positioning System, *J. Appl. Meteor*, 35. 830-838.

Gutman, S.I., R. Pursaud, and S. Wagoner, 2003. Use of federal and state departments of transportation continuously operating GPS reference stations for NOAA weather forecasting, 12th Symposium on Meteorological Observations and Instrumentation, Amer. Meteor. Soc., Long Beach, CA.

Gutman, S.I., S.G. Benjamin, 2001. The Role of Ground-Based GPS Meteorological Observations in Numerical Weather Prediction, GPS Solutions, Volume 4, No. 4, pp. 16-24.

MacDonald, A.E., and Y. Xie, 2000: On the use of slant observations from GPS to diagnose three-dimensional water vapor using 3DVAR. Preprints, Fourth Symposium on Integrated Observing Systems, Long Beach, CA. Amer. Meteor. Soc., 62-73.

Mikhail, E. (1976). Observations and Least Squares. University Press of America.

Miller, P.A., M. F. Barth and L.L. Morone, in preparation. RSAS Technical Procedures Bulletin, Draft-March, 2002.

Niell, A.E., Global mapping functions for the atmospheric delay at radio wavelengths, 1996. *J. Geophys. Res.*, 101,3227-3246.

Ross, R. and S. Rosenfeld, 1997. Estimating mean weighted temperature of the atmosphere for Global Positioning System applications. J. Geophys. Res., Vol. 102, 21,719 - 21,730.

Saastamoinen, J., 1972. Introduction to practical computation of astronomical refraction, Bull. Geod., 106, 383-397.

Smith, T.L., S.G. Benjamin, B.E. Schwartz, B.E., and S.I. Gutman, 2002. Impact of GPS water vapor data on RUC severe weather forecasts. 21st Conference on Severe Local Storms, paper J5.3 (joint session with the NWP/WAF conference) San Antonio, TX Aug. 12-16.

Smith, T.L., S.G. Benjamin, B.E. Schwartz, B.E., and S.I. Gutman, 2000. Using GPS-IPW in a 4-D data assimilation system. Earth, Planets and Space, 52, 921-926.

Smith, T.L., S.G Benjamin, B.E. Schwartz, and S.I. Gutman, 1999. Using GPS-IPW in a 4D data assimilation system, The International Symposium on GPS Application to Earth Sciences (GPS'99 in Tsukuba), October 18-22, Tsukuba, Ibaraki, Japan.